ACS OMEGA

http://pubs.acs.org/journal/acsodf

Article

Surface-Coated Cerium Nanoparticles to Improve Chemotherapeutic Delivery to Tumor Cells

Nilkamal Pramanik,* Tamasa De, Preeti Sharma, Alakesh Alakesh, Sameer Kumar Jagirdar, Annapoorni Rangarajan, and Siddharth Jhunjhunwala

Cite This: *ACS Omega* 2022, 7, 31651−31657

Read Online

ACCESS | Metrics & More | Article Recommendations | Supporting Information

ABSTRACT: The antioxidant property of cerium oxide nanoparticles has increased their demand as a nanocarrier to improve the delivery and therapeutic efficacy of anticancer drugs. Here, we report the synthesis of alginate-coated ceria nanoformulations (ceria NPs) and characterization using FTIR spectroscopy, Raman microscopy, and X-ray diffraction. The synthesized ceria NPs show negligible inherent *in vitro* toxicity when tested on a MDA-MB-231 breast cancer cell line at higher particle concentrations. Upon loading these particles with doxorubicin (Dox) and paclitaxel (PTX) drugs, we observe a potential synergistic cytotoxic effect mediated by the drug and the ceria NPs, resulting in the better killing capacity as well as suppression of cell migration against the MDA-MB-231 cell line. Further, to verify the immune-escaping capacity before targeting cancer cells, we coated the drug-loaded ceria NPs with the membrane of MDA-MB-231 cells using an extrusion method. The resultant delivery system exhibited *in vitro* preferential uptake by the MDA-MB-231 cell line and showed reduced uptake by the murine macrophage cell line (RAW 264.7), assigning its potential application as non-immunogenic personalized therapy in targeting and killing of cancer cells.

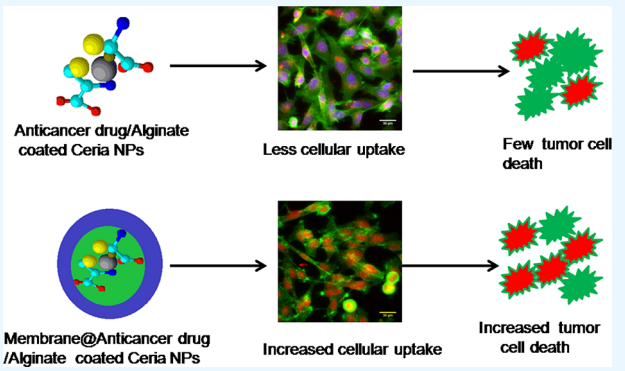

INTRODUCTION

Cerium oxide nanoparticles (ceria NPs) are suggested to have immense potential as a cancer therapeutic.[1] Their mode of action is thought to be through the production of intracellular reactive oxygen species,[2] and hence, they exhibit synergistic cytotoxicity when used with chemotherapeutics.[3] However, a serious concern with the use of ceria NPs is its tendency to agglomerate, which leads to adverse side effects.[4]

To reduce agglomeration, ceria NPs have been coated with biomolecules such as proteins, lipids, and even polysaccharides, which are thought to increase the dispersity in aqueous solutions and hence improve biological activity.[5,6] While such coatings are better than bare particle surfaces, their biological compatibility needs to be improved further. In this context, a technique to reduce agglomeration and enhance cancer cell targeting of nanoparticles (NPs) is to camouflage them using the plasma membrane of cancer cells.[7,8] Unlike simple biopolymer-coated NPs, a biomimetic membrane-coated system may be more attractive as the phospholipid bilayer structure could enable serum stability of nanoparticles.[9] Further, due to the presence of different surface proteins, cancer cell membrane-coated nanoparticles exhibit significant homotypic targeting,[10] cellular uptake, and immune-escape.[11]

In this study, we utilized the approaches of biopolymer as well as cell-membrane coating along with the encapsulation of chemotherapeutics to improve the efficacy of ceria NPs in killing tumor cells. First, we formulated alginate-coated ceria NPs for the delivery of chemotherapeutic agents, doxorubicin (Dox) and paclitaxel (PTX), and demonstrate their performance in killing tumor cells and reducing their migration through *in vitro* studies. Next, we show that coating of the drug-loaded ceria NPs with the cell membranes of cancer cells results in their evasion from uptake by immune cells. There is an unmet need to exploit a potential nanoplatform that would enable us to target the cancer cells with a mechanism of sustained release of therapeutic agents. In our ongoing research, the demonstration of cancer membrane-coated and patient-specific targeted delivery of various anticancer drugs in both *in vitro* and *in vivo* models is targeted.

MATERIALS AND METHODS

Materials. Cerium(III) nitrate hexahydrate [$Ce(NO_3)_3 \cdot 6H_2O$], sodium alginate, 1-ethyl-3(3-dimethylaminopropyl)-

Received: January 4, 2022
Accepted: August 18, 2022
Published: September 1, 2022

carbodiimide hydrochloride (EDAC·HCl), and *N*-hydroxysuccinimide (NHS) were purchased from Merck (USA). Doxorubicin hydrochloride (Dox·HCl, henceforth referred to as Dox) and dimethyl sulfoxide (DMSO) were obtained from Merck (India) and paclitaxel (PTX) from SRL Chemicals (India). All cell culture reagents were purchased from Lonza Biosciences (India). To compare particles prepared by us to a standard control, cerium oxide [IV] nanoparticles were purchased from Merck (USA).

Synthesis of Alginate-Coated Cerium Nanoparticles [CeO_2NPs (Ceria NPs)]. To formulate a colloidal solution of ceria nanoparticles in water, 15 mg of sodium alginate was dissolved in 10 mL of MES buffer (pH 5.4). The alginate polymer was first incubated with 5 mg of EDAC·HCl and 6.5 mg of NHS for 2 h. Next, 0.4 g of cerium nitrate salt was added to the EDAC·HCl/NHS activated alginate solution under stirring at 37 °C. This was followed by the dropwise addition of ammonium hydroxide until the solution turned dark brown. After 24 h of reaction, the solution was centrifuged at 16000 rcf for 10 min and the pellet was washed twice using distilled water. Finally, the solution was sonicated for 2 h to generate aqua-dispersed alginate-coated ceria nanoparticles. These particles were stored at 4 °C till further use. These particles will be referred to as "Insitu ceria". Similarly, 10 mg of cerium oxide nanoparticles (purchased from Merck) was finely dispersed into 2 mL of 1% alginate solution under ultrasonication [50% amplitude, 125 Watts, 20 KHz] for 2 h, centrifuged at 3600 rcf for 10 min to remove the debris, and stored at 4 °C till further use. These particles will be referred to as "Post coating ceria". The concentration of the ceria NPs present in each nanoformulation was calculated using a standard absorbance calibration curve at 295 nm prepared by the serial dilution of native ceria NPs.

Loading of Anticancer Drugs. To load chemotherapeutic agents, 500 μM doxorubicin hydrochloride (Dox) and paclitaxel were separately added to 200 μL of 1 mg/mL 1× PBS solution of Insitu ceria and Post coating ceria, and the system was kept at room temperature in the dark under stirring for 15−16 h. Particles were then centrifuged at 16000 rcf for 10 min, and the pellet was washed twice to remove the non-adsorbed drugs. Loading efficiency was calculated using a UV−visible spectrophotometer by measuring the absorbance at 231 nm for PTX and 488 nm for Dox after centrifugation of the drug-loaded ceria NPs at 16000 rcf. The concentration of the drugs in the supernatant was calculated using the standard calibration curve, and the residual amount of drug in the supernatant from both washes was used to calculate the quantity of adsorbed drugs (total drug added minus the sum of the drug content in the supernatant of the two washes). Adsorption of drugs onto ceria NPs was also confirmed using FTIR spectral analysis.

Formulation of MDA-MB-231 Membrane-Coated Ceria Nanoparticles [Mem@Ceria NPs]. Camouflaged nanoparticles were prepared using an extrusion method,[11] which enabled the coating of cell membranes on nanoparticles. In brief, the MDA-MB-231 breast cancer cell line was first treated with hypotonic solution [8 mM Tris−HCl buffer (pH 7.4) and 3 mM EDTA] for 1 h on ice (0−4 °C) and then homogenized at 20000 rpm for 60 s. Cell organelles were then isolated as a pellet through centrifugation of the cell lysate at 700*g* for 10 min. The supernatant was further centrifuged at 16000 rcf for 30 min at 0−4 °C. The second supernatant was discarded, and the pellet was washed twice with 1× PBS and sonicated for 10 s. Finally, the resulting suspension was mixed with nanoceria or drug (1 mM) [Dox or PTX]-loaded nanoceria and sonicated for 10 min under ice-cold conditions. Then, it was extruded nine times through a series of (1, 0.4, and 0.2 μM) polycarbonate porous membranes to obtain size-controlled cell membrane-coated ceria nanoparticles. The camouflaged systems, i.e., membrane-coated in situ ceria nanoparticles [Mem@Insitu CeO_2NPs], membrane-coated post-coating ceria nanoparticles [Mem@Post CeO_2NPs], membrane-coated Dox- or PTX-loaded in situ ceria nanoparticles [Mem@Dox-Insitu Ceria NPs or Mem@PTX-Insitu Ceria NPs], and membrane-coated Dox- or PTX-loaded post-coating ceria nanoparticles [Mem@Dox-Post-coating ceria NPs or Mem@PTX-Post-coating ceria NPs] were stored at 4 °C until further use.

The extent of protein in the cell membrane was assessed using a bicinchoninic acid (BCA) protein assay kit. A 10 μL sample solution was added to 96 well-microplates followed by the addition of 90 μL of BCA reagent. The plate was incubated for 2 h at 37 °C in the dark, and the violet solution's absorbance was recorded at 562 nm to quantify the protein concentration using a BSA standard curve.

Characterization of Ceria Nanoparticles. The cerium−oxygen bond stretching of the synthesized different ceria nanoparticles were analyzed using Fourier transform infrared spectroscopy [FTIR, PerkinElmer FTIR spectrometer (model: L1860121 USA), scanning from 4000 to 500 cm^{-1} for 42 consecutive scans at room temperature] and Raman microscopy at 532 nm laser [Lab RAM HR]. The hydrodynamic radius and surface charge of the particles were recorded using a Zetasizer Nano ZS dynamic light-scattering (DLS) instrument (Malvern, UK) at room temperature. The surface morphology and elemental composition of the different ceria NPs were investigated using scanning electron microscopy [FESEM, JEOL, Germany] and high-resolution transmission electron microscopy [TEM, Titan THEMIS, 300 KeV]. The diffraction pattern of the ceria NPs was evaluated through powder X-ray diffraction [XRD] [Rigaku, filtered CuKα radiation operated at 40 kV and 30 mA over the range of 2θ = 5−90°].

***In Vitro* Drug Release Study.** To evaluate the *in vitro* drug release profile of drug molecules from the ceria NPs system at pH 5.4 (endosomal pH) and pH 7.4 (cytosolic pH), doxorubicin hydrochloride/PTX-loaded ceria NPs were selected, and release kinetics were determined. Briefly, Dox [0.5 mM]-loaded ceria NPs or membrane-coated Dox [0.5 mM]-loaded ceria NPs were incubated in 1 mL of sodium acetate buffer [pH 5.4] and phosphate buffer saline [(PBS, serum condition, i.e., PBS + 1%BSA) pH 7.4] at 37 °C under shaking conditions. At various time points, the particles were centrifuged at 16000 rcf for 10 min and 160 μL of the supernatant was withdrawn and replaced with the same volume of fresh buffer. Finally, the percentage of drug present in the supernatant was measured using a UV−visible spectrophotometer. Similarly, the "*in vitro*" release profile of PTX from PTX/ceria NPs was conducted at pH 7.4.

***In Vitro* Cellular Internalization of Ceria Nanoparticles.** In order to investigate the intracellular uptake of different ceria nanoparticles, 5 × 10^4 MDA-MB-231 breast cancer cell lines were seeded into 12-well plates and incubated for 12 h at 37 °C in the presence of 5% CO_2 under humidified conditions. Next, Dox-loaded nanoceria (at a Dox concentration of 5 μM) was added to cells and incubated for another

https://doi.org/10.1021/acsomega.2c00062
ACS Omega 2022, 7, 31651−31657

4 h. Finally, the uptake of nanoparticles was tracked using a fluorescence microscope (Incell analyzer 6000, GE, USA).

The uptake of membrane-coated ceria nanoparticles was also monitored in the presence of a murine macrophage cell line Raw 264.7 to verify the evasion ability from immune cells. The cells were incubated with 5 μM Dox-loaded ceria NPs for 4 h. Then, the cells were washed once with PBS and the uptake was recorded through a fluorescence microscope and using a flow cytometer.

***In Vitro* Toxicity Assays.** The inherent toxicity of native ceria NPs, Insitu ceria NPs, and Post-coating ceria NPs was assessed to investigate the threshold values of particle concentration above that shows an adverse effect on cells. Briefly, MDA-MB-231 cells were seeded in a 96-well plate at a density of 5×10^3 cells per well. After overnight incubation, cells were treated with different concentrations [100, 50, 25, 12.5, 6.25, and 3.13 μg/mL] of ceria NPs in DMEM media for another 24 h. Finally, the MTT assay (Merck, USA) was used to determine the percentage of cell viability.

The chemotherapeutic efficiency of the anticancer drugs [Dox (5 μM and its serial diluted solution) and PTX (100 nM and its serial diluted solution)] was evaluated by the encapsulation of the drugs into nanoceria [both Insitu ceria NPs and Post-coating ceria NPs] followed by the addition of the particles to MDA-MB-231 cells and incubating for 48 h. The percentage of cell viability was calculated with respect to untreated cells.

Cell Migration Assays. Cell motility was determined to monitor the migration capability of breast cancer cells [MDA-MB-231] in the presence of paclitaxel (PTX) (a tubulin-binding drug) and their nanoparticle formulations. Cells at a concentration of 5×10^4 cells were initially seeded onto 24-well plates and incubated until cells reached around 80−90% of the surface of the plates. Then, a vertical scratch was created using a sterilized 200 μL tip and cell debris was removed by washing. Different concentrations [(100, 50, 25, and 12.5 nM PTX/PTX-ceria NPs) and (5, 2.5, 1.25, and 0.615 μM Dox/Dox-ceria/m@DoxNPs)] of anticancer drugs and their nanoparticle combination were added to each well. Similarly, a vehicle control experiment was also conducted in the presence of ceria NPs (15, 7.5, and 3.75 μg/mL). The wound area was recorded using a stereo-microscope after 24 and 48 h of incubation. Finally, the percentage of wound contraction was calculated using Image J.

Statistical Analysis. All chemical syntheses and characterizations were repeated at least twice. For biological studies, at least three independent experiments were performed, and mean ± S.D. of the data was reported. The statistical significance was calculated using two-way ANOVA or one-way ANOVA followed by Bonferroni Multiple Comparisons test [*p < 0.05, **p < 0.01, ***p < 0.001, and ****p < 0.0001].

RESULTS AND DISCUSSION

Characterization of Nanoceria. First, ceria NPs were coated with alginate using two different methods, resulting in the generation of Insitu ceria NPs and Post coating ceria NPs. The size and charge of the ceria NPs were determined using dynamic light scattering. Insitu and Post coating ceria NPs were found to be of comparable size and surface charge (Table 1).

Confirmation of the size and morphology of particles was obtained through scanning and transmission electron microscopy (Figures S1 and S2). To determine the composition of the particles, UV−visible spectroscopy and FTIR spectroscopy were performed. The UV−visible spectra of the particles showed strong absorption bands in the range of 290−300 nm, which may be attributed to the ligand (O 2p) to metal (Ce 4f) charge transfer in ceria nanoparticles[12] (Figure 1a). The absorption in this region appeared to be enhanced upon coating with alginate. FTIR spectral analysis of the Post coating and Insitu ceria as well as the control nanoparticles and sodium alginate is shown in Figure 1b. The presence of a band at 570−590 cm^{-1} is likely to be due to the Ce−O stretching, 3350−3400 cm^{-1} is due to the −OH stretching, and ∼1600 cm^{-1} is possibly due to the $-COO^-$ stretching, all of which confirm the synthesis of alginate-coated ceria NPs. These data are in agreement with a previous report.[13]

Table 1. DLS Hydrodynamic Size and Zeta Potential Values of Different Ceria NPs

nanoparticulates	size (nm)	zeta potential (−mV)	polydispersity index (PDI)
Post coating ceria NPs	77.55 ± 0.51	20.9 ± 2.33	0.228 ± 0.008
Insitu ceria NPs	75.37 ± 6.95	17.43 ± 1.06	0.27 ± 0.074

Further analysis of these particles was performed using Raman and XRD spectroscopy. The Raman spectra (Figure 2a) showed a peak around 460 cm^{-1}, which is likely due to the symmetrical stretching vibration mode of the Ce-O_8 unit in a ceria nanocrystal.[14] Additional Raman bands around 1100 cm^{-1} in alginate-coated NPs indicated the presence of a carbonaceous material. X-ray diffraction patterns [XRD, Figure 2b] of the fabricated polymer-coated ceria NPs and membrane-coated ceria NPs also indicated nearly similar diffraction peaks at 28° (Miller indices, hkl = 111), 32.7° (Miller indices, hkl = 200), 47° (Miller indices, hkl = 220), and 56° (Miller indices, hkl = 311), which is in agreement with a previous report.[15] However, as compared to ceria NPs, polymer- or membrane-coated ceria NPs showed broader peaks. These characterizations demonstrated the successful coating of ceria NPs with alginate.

Drug Loading and Release Study. To investigate the drug-carrying capability of the particles, simple adsorption was employed to load the two drugs, doxorubicin (Dox) and paclitaxel (PTX). The ratios of the mass of the drug molecules adsorbed to the amount of drug-loaded NPs [i.e., DLE = wt. of drug/(wt. of drug + wt. of NPs)] were calculated to be 31.71 ± 3.028% (Insitu ceria@Dox), 35.53 ± 6.02% (Post-coating ceria@Dox), 16.23 ± 8.11% (Insitu@PTX), and 14.7 ± 8.4% (Post-coating ceria@PTX). Similarly, loading percentages of ceria in ceria/drug nanoformulations were calculated to be 68.29 ± 3.03% (Insitu ceria@Dox), 64.47 ± 6.024% (Post-coating ceria@Dox), 83.77 ± 7.86% (Insitu@PTX), and 85.30 ± 8.41% (Post-coating ceria@PTX). Moreover, the drug encapsulation efficiencies [DEE] were measured as 80.43 ± 10.98% (Insitu ceria@Dox), 86.75 ± 11.66% (Post-coating ceria@Dox), 22.06 ± 9.91% (Insitu@PTX), and 21.15 ± 12.92% (Post-coating ceria@PTX). We speculate that the differences in encapsulation efficiencies of the two drugs could be due to noncovalent interactions between the materials and the drug.

UV−visible spectra [Figure S3a,b] and FTIR spectra analyses [Figure S4a,b] of the drug-loaded ceria NPs also confirmed the successful entrapment of drug molecules. *In vitro* drug release kinetics of doxorubicin was investigated at

https://doi.org/10.1021/acsomega.2c00062
ACS Omega 2022, 7, 31651−31657

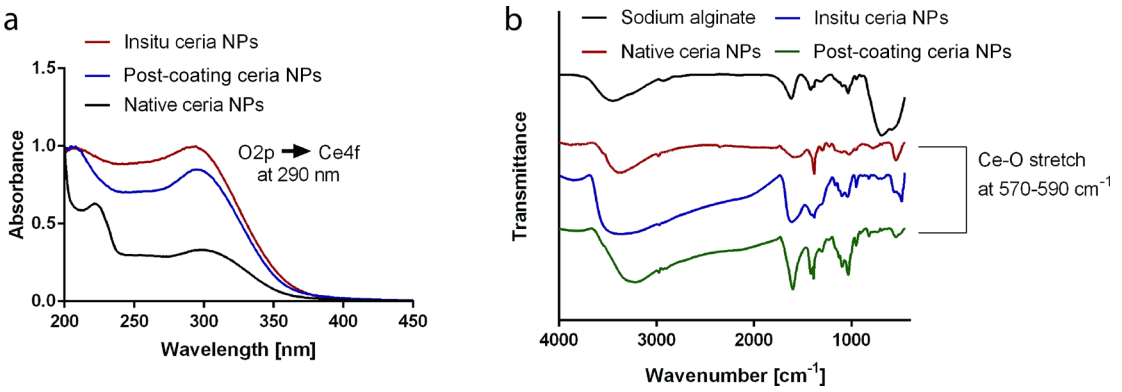

Figure 1. UV−Visible and FTIR spectroscopy. (a) UV−visible absorbance scans from 200 to 450 nm of different nanoceria showing characteristic cerium peaks between 290 and 300 nm. (b) FTIR spectroscopy of sodium alginate, native ceria NPs, Insitu alginate-coated ceria NPs, and Post coating ceria NPs, showing the characteristic Ce−O stretch at 550−570 cm^{-1} and other peaks at 1620 and 3350−3400 cm^{-1}, confirming the synthesis of polymer-coated ceria NPs.

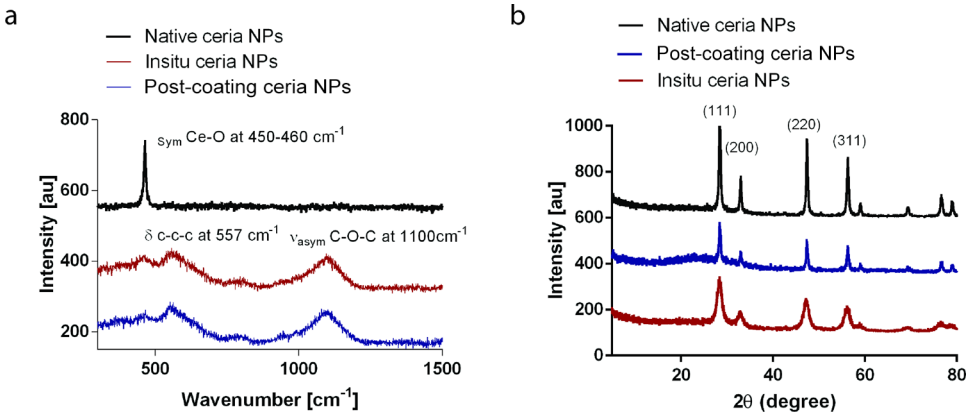

Figure 2. (a) Raman microscopy analysis of different ceria nanoparticles. Characteristic peaks at 450 and 557 cm^{-1} were observed in different ceria nanoparticles, confirming the presence of Ce−O in the synthesized nanoparticles. (b) XRD spectroscopy analysis of different ceria nanoparticles. The peaks (2 theta values) at 30° (111), 46° (220), and 58° (311) reveal the presence of crystalline nanoceria.

pH 5.4 (endosomal pH) and 7.4 (cytosolic pH). We observed that the release was faster at the lower pH (5.4) with nearly 40% of the drug released in the first 10 h, while the release was slower at the higher pH (7.4) with and without serum protein with about 28 and 25% drug released in the first 10 h, respectively (Figure S5a). As a consequence, over a 2 day period (48 h), about 60% of the drug was released at the lower pH when compared to about 20% released at the higher pH in the same time-frame.

In contrast, alginate@PTX-ceria NPs exhibited 35% of cumulative PTX release under the serum condition at pH 7.4 after 48 h of incubation (Figure S5b). Like the Dox-ceria system, the lower release rate of PTX at pH 7.4 (Figure S5b) indicates the coverage of PTX molecules by the alginate coating, which could be beneficial for the targeted delivery of the drug with a minimum spreading in blood plasma.

Cell Cytotoxicity Assays. To test the compatibility of ceria NP in the absence of a drug, we measured their effect on cell survival following co-incubation with cells. None of the NPs showed any significant cytotoxicity at a low particle concentration [<25 μg/mL], but around 30−35% of cell death was observed at a higher concentration [100 μg/mL] (Figure 3a). The cytotoxicity observed at a high concentration may be due to the antioxidant property of ceria NPs that triggers the activation of caspase-3 signaling pathways, resulting in significant cell death.[16] Hence, for all further studies, we used a lower particle concentration to avoid cytotoxicity due to NPs themselves.

Next, the dose-dependent effect of Dox- and PTX-loaded ceria NPs was investigated using the MDA-MB-231 cell line. In these studies, the dose of each NPs used was 15 μg/mL. For Dox-NPs, the post-coating technique resulted in higher tumor cell killing capacities at a low drug concentration compared to native drug solution, and the Insitu ceria NPs did not show significant differences (Figure 3b). For PTX-NPs, both particle formulations showed a better killing capacity at low drug concentrations relative to native drug solution (Figure 3c). The exact reasons behind the different trends observed for Dox and PTX-NPs remain unclear, but Post coating ceria NPs (for both drugs) showed superior efficacy at cell killing at a low drug concentration compared to Insitu drugs/ceria NPs.

Cell Migration and Invasiveness Assays. Following the demonstration of *in vitro* cell killing, we next determined the effect of drug-loaded ceria NPs on cell migration. In the case of PTX drug treatment, the PTX-ceria NPs were found to significantly inhibit the migration of MDA-MB-231 cells as compared to only the PTX drug or ceria NPs as a vehicle control (Figure 4b,c and Figure S6a). After 48 h of incubation, both PTX-Insitu and PTX-Post-coating ceria NPs demonstrated a 1.7-fold and 1.9-fold higher area closure as compared to only PTX drugs [Figure S6b], indicating significant inhibition of cell migration. The superior tubulin binding

https://doi.org/10.1021/acsomega.2c00062
ACS Omega 2022, 7, 31651−31657

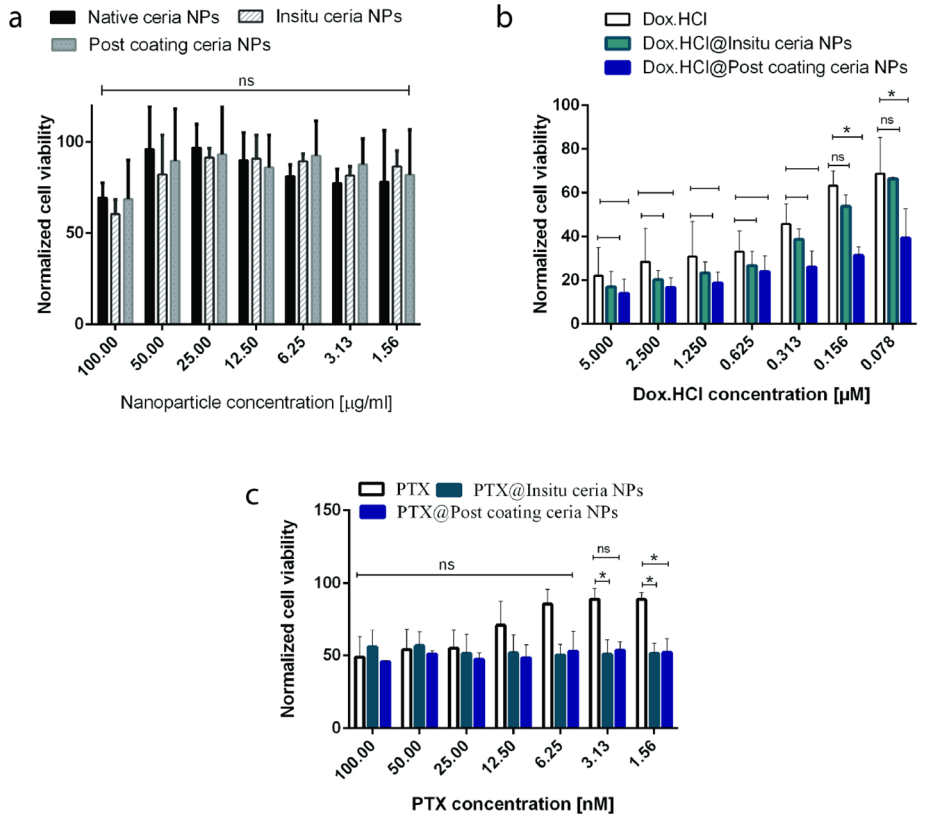

Figure 3. *In vitro* cytotoxicity assays of (a) different ceria NPs, (b) DOX-loaded ceria NPs, and (c) PTX-loaded ceria NPs. Varying concentrations of each particulate were cultured with MDA MB231, and their effect on cell viability was measured. The percentages of cell viability were normalized to the control cell cultures in completely particle-free media. Each data point represents mean ± standard deviation [$N = 3$]. The statistical significance was calculated using two-way ANOVA followed by a Bonferroni Multiple Comparisons test [$^{*}p < 0.05$, $^{**}p < 0.01$, $^{***}p < 0.001$, and $^{****}p < 0.0001$].

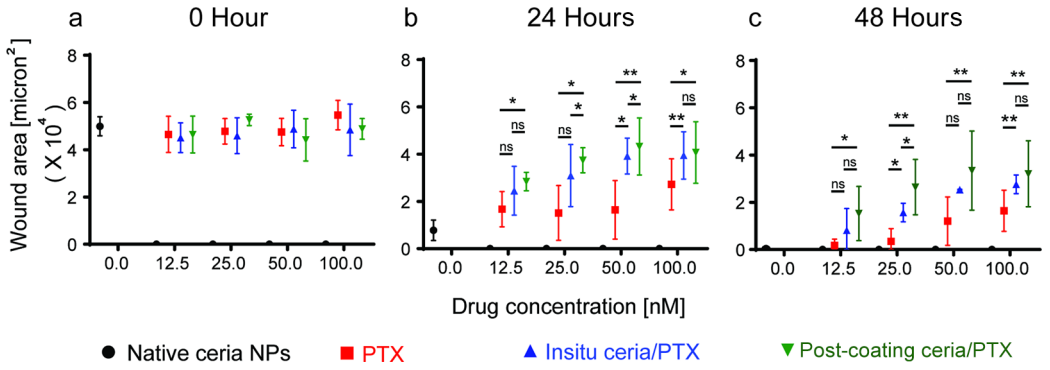

Figure 4. Plot of *in vitro* MDA-MB-231 cell migration at (a) (initial time point) 0 h, (b) 24 h, and (c) 48 h in the presence of only PTX drug and PTX loaded in different ceria NPs. Each data point represents mean ± standard deviation [$N = 3$]. The area of cell migration was captured through a Stero-microscope at 10× objective. Image J software was used to calculate the area of cell migration. One-way ANOVA followed by a Bonferroni post test is performed to compare the effect of PTX on cell migration with cell control [$^{*}p < 0.05$, $^{**}p < 0.01$, $^{***}p < 0.001$, and $^{****}p < 0.0001$].

ability of PTX[17] may cause the changes in cell migration that we observed in our studies. Unlike PTX-ceria NPs, Dox-ceria NPs caused the death of adherent cells in culture at a higher DOX concentration [5 μM] [Figure S7].

Membrane-Coated Ceria NPs. Nanoparticles tend to be cleared by phagocytic immune cells, which results in a low accumulation of particles in the tumor microenvironment. Cell membrane coating has been suggested to be a useful strategy in improving cell targeting while also ensuring that uptake by immune cells is avoided. Hence, we coated the ceria NPs with cell membranes of MDA-MB-231 cells using techniques demonstrated by others.[4,12] The average hydrodynamic radii of Mem@Insitu ceria NPs and Mem@Post-coating ceria NPs were found to be 123.43 ± 0.6 and 140 ± 0.2 nm, respectively. The zeta potential values were obtained as −9.63 ± 1.8 and −15.53 ± 0.90 mV, respectively, as shown in Table 2. As compared to the naked spherical structure, the larger size of Mem@ceria NPs is due to the additional outer phospholipid bilayer membrane, resulting in the spherical core−shell geometry that is confirmed by high-resolution transmission electron microscopy analysis, as shown in Figure S8. The selected area electron diffraction (SAED) analysis reveals the

https://doi.org/10.1021/acsomega.2c00062
ACS Omega 2022, 7, 31651−31657

Table 2. DLS Hydrodynamic Size and Zeta Potential Values of Different Membrane-Coated and Drug-Loaded Ceria NPs

nanoparticulates	size (nm)	zeta potential (−mV)	polydispersity index (PDI)
Mem@Dox-Insitu ceria NPS	123.43 ± 0.6	9.63 ± 1.83	0.34 ± 0.014
Mem@Dox-Post-coating ceria NPs	140 ± 0.2	15.53 ± 0.90	0.288 ± 0.0138
Mem@PTX-Insitu ceria NPs	115.83 ± 0.97	14.66 ± 3.4	0.327 ± 0.043
Mem@PTX-Post-coating ceria NPs	127.06 ± 1.5	9.82 ± 2.75	0.3 ± 0.078

Debye−Scherrer diffraction rings due to the cubic fluorite crystal structure of a ceria nanocrystal.[18]

The hydrodynamic size of the NPs is larger than the size observed in TEM images. The larger hydrodynamic size of the NPs may be due to the slight aggregation of the NPs with additional hydration layers.

Again, the results of the BCA assay showed the presence of a significant amount of membrane-specific proteins in Mem@alginate-ceria NPs, Mem@alginate/Dox ceria NPs, and Mem@alginate/PTX-ceria NPs, as shown in Figure S9, which confirms the presence of the cell membrane on various ceria nanoformulations.

In vitro release kinetics of Dox was altered slightly following membrane coating (Figure S10). At the initial time points, the pH condition triggered a similar trend of release percentage [7−15%] in both membrane-coated and alginate-coated ceria NPs. However, over 2 days, the membrane-coated ceria NPs [Mem@ceria NPs] released around 20−30% of Dox, whereas 50−60% was released in the alginate-coated particles [Figure S5a]. The slower release could be attributed to the membrane, which lowers the diffusion rates of the drug molecule. Phospholipids present a significant diffusion barrier to the release of drugs, and hence a nanoformulation coated with phospholipid membranes is likely to have a lower release rate.[19] We also speculate that there may be electrostatic interactions between the cell membrane (negatively charged) and the positively charged drug molecules, which could alter release rates.

Next, the membrane-coated particles were tested for their ability to be taken up by the MDA-MB-231 cancer cells. Membrane-coated ceria NPs were taken up into the cancer cells at significantly higher levels [Figure S12a,b] when compared to non-coated ceria NPs [Figure S11a]. To determine the ability to avoid immune cell uptake, particles were incubated with RAW 264.7 macrophages. A decreased uptake of membrane-coated ceria NPs was observed [Figure S13a,b] as compared to non-coated particles [Figure S11b] by confocal microscopy. The significant uptake of coated nanoparticles as compared to the non-coated system by cancer cells would be favorable as a potential nanovehicle for prolonged therapeutic action of anticancer drugs in targeted cancer therapy. However, further work is required in the future to determine the extent of evasion of uptake by immune cells.

CONCLUSIONS

Herein, we used two different methods to formulate alginate-coated and cell membrane-coated ceria NPs successfully. The inherent cytotoxicity of these particles was found to be negligible, especially at low concentrations. Chemotherapeutic drugs could be loaded onto both types of ceria NPs, and drug release kinetics was measured. Through *in vitro* tests involving the MDA-MB-231 cell line, we show that the drug-loaded ceria NPs are better at cell killing as compared to free chemotherapeutic drugs. Further, the cell membrane-coated ceria NP system showed reduced uptake by macrophages *in vitro*, suggestive of its ability to evade the immune cells, underlying its acceptance as a potential nanovehicle for prolonged therapeutic action of anticancer drugs in targeted cancer therapy. Together, these data suggest that the drug-loaded and membrane-coated ceria NPs have the potential to be used as an anticancer therapeutic with possibly increased tumor targeting due to the immune evasion capacity.

ASSOCIATED CONTENT

Supporting Information

The Supporting Information is available free of charge at https://pubs.acs.org/doi/10.1021/acsomega.2c00062.

SEM, TEM, and FTIR and UV−visible spectra analysis of various ceria NPs, *in vitro* drug release study of Dox-ceria NPs, *in vitro* cell migration, TEM analysis of membrane-coated ceria NPs, doxorubicin drug release profile from different membrane-coated ceria NPs, confocal microscopy analysis of MDA-MB-231 and raw cell uptake, and flow cytometric analysis of cellular uptake [PDF]

AUTHOR INFORMATION

Corresponding Author

Nilkamal Pramanik − *Centre for BioSystems Science and Engineering, Indian Institute of Science, Bengaluru, Karnataka 560012, India;* orcid.org/0000-0003-3042-5555; Email: nilkamal.can@rediffmail.com

Authors

Tamasa De − *Department of Molecular Reproduction, Development and Genetics, Indian Institute of Science, Bengaluru, Karnataka 560012, India*

Preeti Sharma − *Centre for BioSystems Science and Engineering, Indian Institute of Science, Bengaluru, Karnataka 560012, India*

Alakesh Alakesh − *Centre for BioSystems Science and Engineering, Indian Institute of Science, Bengaluru, Karnataka 560012, India*

Sameer Kumar Jagirdar − *Centre for BioSystems Science and Engineering, Indian Institute of Science, Bengaluru, Karnataka 560012, India;* orcid.org/0000-0002-6200-5590

Annapoorni Rangarajan − *Department of Molecular Reproduction, Development and Genetics, Indian Institute of Science, Bengaluru, Karnataka 560012, India*

Siddharth Jhunjhunwala − *Centre for BioSystems Science and Engineering, Indian Institute of Science, Bengaluru, Karnataka 560012, India;* orcid.org/0000-0001-8046-2288

Complete contact information is available at: https://pubs.acs.org/10.1021/acsomega.2c00062

Notes

The authors declare no competing financial interest.

■ ACKNOWLEDGMENTS

This work was supported by a National Postdoctoral Fellowship to N.P. (PDF/2016/001685) and Ramanujan Fellowship to S.J. (SB/S2/RJN-135/2015) from the Science and Engineering Board, Department of Science and Technology, Government of India. DBT-IISc Partnership Program Phase-II (BT/PR27952-INF/22/212/2018) is acknowledged for infrastructure and financial support to A.R.

■ REFERENCES

(1) Asati, A.; Santra, S.; Kaittanis, C.; Perez, J. M. Surface-Charge-Dependent Cell Localization and Cytotoxicity of Cerium Oxide Nanoparticles. *ACS Nano* **2010**, *4*, 5321−5331.

(2) Korsvik, C.; Patil, S.; Seal, S.; Self, W. T. Superoxide Dismutase Mimetic Properties Exhibited by Vacancy Engineered Ceria Nanoparticles. *Chem. Commun.* **2007**, *10*, 1056−1058.

(3) *Sack M1, Alili L2, Karaman E2, Das S3, Gupta A3, Seal S3, Brenneisen P2. Combination of conventional chemotherapeutics with redox-active cerium oxide nanoparticles--a novel aspect in cancer therapy.* PubMed NCBI https://www.ncbi.nlm.nih.gov/pubmed/24825856 (accessed 2019−04 -20).

(4) Heckman, K. L.; Estevez, A. Y.; DeCoteau, W.; Vangellow, S.; Ribeiro, S.; Chiarenzelli, J.; Hays-Erlichman, B.; Erlichman, J. S. Variable in Vivo and in Vitro Biological Effects of Cerium Oxide Nanoparticle Formulations. *Front. Pharmacol.* **2020**, *10*, 1599.

(5) Mukherjee, A.; Madamsetty, V. S.; Paul, M. K.; Mukherjee, S. Recent Advancements of Nanomedicine towards Antiangiogenic Therapy in Cancer. *Int. J. Mol. Sci.* **2020**, *21*, 455.

(6) Abuid, N. J.; Gattás-Asfura, K. M.; Schofield, E. A.; Stabler, C. L. Layer-by-Layer Cerium Oxide Nanoparticle Coating for Antioxidant Protection of Encapsulated Beta Cells. *Adv. Healthcare Mater.* **2019**, *8*, 1801493.

(7) Yang, R.; Xu, J.; Xu, L.; Sun, X.; Chen, Q.; Zhao, Y.; Peng, R.; Liu, Z. Cancer Cell Membrane-Coated Adjuvant Nanoparticles with Mannose Modification for Effective Anticancer Vaccination. *ACS Nano* **2018**, *12*, 5121−5129.

(8) Li, S.-Y.; Cheng, H.; Xie, B.-R.; Qiu, W.-X.; Zeng, J.-Y.; Li, C.-X.; Wan, S.-S.; Zhang, L.; Liu, W.-L.; Zhang, X.-Z. Cancer Cell Membrane Camouflaged Cascade Bioreactor for Cancer Targeted Starvation and Photodynamic Therapy. *ACS Nano* **2017**, *11*, 7006−7018.

(9) Chen, Z.; Zhao, P.; Luo, Z.; Zheng, M.; Tian, H.; Gong, P.; Gao, G.; Pan, H.; Liu, L.; Ma, A.; Cui, H.; Ma, Y.; Cai, L. Cancer Cell Membrane-Biomimetic Nanoparticles for Homologous-Targeting Dual-Modal Imaging and Photothermal Therapy. *ACS Nano* **2016**, *10*, 10049−10057.

(10) Hu, Q.; Sun, W.; Qian, C.; Wang, C.; Bomba, H. N.; Gu, Z. Anticancer Platelet-Mimicking Nanovehicles. *Adv. Mater.* **2015**, *27*, 7043−7050.

(11) Li, S.-Y.; Cheng, H.; Qiu, W.-X.; Zhang, L.; Wan, S.-S.; Zeng, J.-Y.; Zhang, X.-Z. Cancer Cell Membrane-Coated Biomimetic Platform for Tumor Targeted Photodynamic Therapy and Hypoxia-Amplified Bioreductive Therapy. *Biomaterials* **2017**, *142*, 149−161.

(12) Elaheh, K. *GoharshadiabSaraSamieeaPaulNancarrow. Fabrication of cerium oxide nanoparticles: Characterization and optical properties* - ScienceDirect https://www.sciencedirect.com/science/article/pii/S0021979711000944?via%3Dihub (accessed 2019−04 -18).

(13) Gao, Y.; Chen, X.; Liu, H. A Facile Approach for Synthesis of Nano-CeO_2 Particles Loaded Co-Polymer Matrix and Their Colossal Role for Blood-Brain Barrier Permeability in Cerebral Ischemia. *J. Photochem. Photobiol., B* **2018**, *187*, 184−189.

(14) Hemalatha, K. S.; Rukmani, K. Synthesis, Characterization and Optical Properties of Polyvinyl Alcohol−Cerium Oxide Nanocomposite Films. *RSC Adv.* **2016**, *6*, 74354−74366.

(15) Diaconeasa, Z.; Barbu-Tudoran, L.; Coman, C.; Leopold, L.; Mesaros, A.; Pop, O. L.; Rugina, D.; Stefan, R.; Tabaran, F.; Tripon, S.; Socaciu, C. Cerium Oxide Nanoparticles and Its Cytotoxicity Human Lung Cancer Cells. *Romanian Biotechnological Letters* **2015**, *20*, 10679−10687.

(16) Giri, S.; Karakoti, A.; Graham, R. P.; Maguire, J. L.; Reilly, C. M.; Seal, S.; Rattan, R.; Shridhar, V. Nanoceria: A Rare-Earth Nanoparticle as a Novel Anti-Angiogenic Therapeutic Agent in Ovarian Cancer. *PLoS One* **2013**, *8*, No. e54578.

(17) Leung, J. C.; Cassimeris, L. Reorganization of Paclitaxel-Stabilized Microtubule Arrays at Mitotic Entry: Roles of Depolymerizing Kinesins and Severing Proteins. *Cancer Biol. Ther.* **2019**, *20*, 1337−1347.

(18) Kim, N.-W.; Lee, D.-K.; Yu, H. Selective Shape Control of Cerium Oxide Nanocrystals for Photocatalytic and Chemical Sensing Effect. *RSC Adv.* **2019**, *9*, 13829−13837.

(19) Sun, H.; Su, J.; Meng, Q.; Yin, Q.; Chen, L.; Gu, W.; Zhang, P.; Zhang, Z.; Yu, H.; Wang, S.; Li, Y. Cancer-Cell-Biomimetic Nanoparticles for Targeted Therapy of Homotypic Tumors. *Adv. Mater.* **2016**, *28*, 9581−9588.

https://doi.org/10.1021/acsomega.2c00062
ACS Omega 2022, 7, 31651−31657